

This is the peer reviewed version of the following article:

Enhancing ophthalmic examinations with real-time eye position monitoring using SVM / Gibertoni, Giovanni; Rovati, Luigi. - In: PROGRESS IN BIOMEDICAL OPTICS AND IMAGING. - ISSN 1605-7422. - 13300:(2025). ( Ophthalmic Technologies XXXV 2025 San Francisco, California, United States 25-27 January 2025) [10.1117/12.3044486].

SPIE

*Terms of use:*

The terms and conditions for the reuse of this version of the manuscript are specified in the publishing policy. For all terms of use and more information see the publisher's website.

13/05/2026 22:37

(Article begins on next page)

# Enhancing Ophthalmic Examinations with Real-Time Eye Position Monitoring Using SVM

Giovanni Gibertoni<sup>a,b</sup> and Luigi Rovati<sup>a</sup>

<sup>a</sup>Department of Biomedical, Metabolic and Neural Sciences, University of Modena and Reggio Emilia, Italy

<sup>b</sup>Department of Engineering "Enzo Ferrari", University of Modena and Reggio Emilia, Italy

## ABSTRACT

This work proposes *OptoCheck*, a modular and compact solution to monitor eye state and patient cooperation during ophthalmic exams. Our solution integrates an optical architecture, including a CMOS board-level camera and a dichroic mirror, and employs a Support Vector Machine (SVM)-based classification algorithm for real-time image analysis. The system is engineered to be compatible with current ophthalmic instruments, such as pupillometers and Optical Coherence Tomography (OCT), with minimal modifications. We tested the system on eight healthy subjects to evaluate its ability to detect eye movements, blinks, and small misalignments in real time. This approach improves the reliability of ophthalmic tests, shortens examination times, and supports more accurate and timely diagnoses, particularly in settings involving non-cooperative patients, such as pediatric or geriatric cases.

## 1. INTRODUCTION

The integration of Artificial Intelligence (AI) into medical equipment is becoming increasingly popular.<sup>1,2</sup> Artificial intelligence applied to fields such as computer vision, machine learning (ML), and deep learning (DL) has improved traditional medical instrumentation.<sup>3,4</sup> In particular, AI has significantly advanced biomedical imaging,<sup>5</sup> ocular data analysis,<sup>6,7</sup> and ophthalmic image analysis.<sup>8</sup> Digital cameras have significantly improved diagnostics and the detection of disease progression.<sup>9</sup> Procedures such as slit lamp microscopy,<sup>10,11,12</sup> Optical Coherence Tomography (OCT),<sup>13</sup> funduscopy,<sup>14</sup> and pupillometry<sup>4,15</sup> benefit from these advancements. Despite these advancements, ophthalmic measurements still face significant challenges, particularly with non-cooperative patients such as children, elderly individuals, or those with physical or cognitive impairments. For example, visual field tests and intraocular pressure (IOP) measurements can be compromised by patient movement, reduced attention spans, or discomfort.<sup>16</sup> These limitations emphasize the importance of adaptive systems to maintain diagnostic accuracy under challenging conditions.<sup>17</sup> Several studies have explored vision-based algorithms to mitigate these challenges, focusing on enhancing data acquisition reliability during ophthalmic tests.<sup>2,18</sup> Real-time image filtering and eye position recognition techniques have demonstrated significant potential for improving diagnostic reliability.<sup>19</sup> For example, AI-driven classification methods for pupil alignment and blink detection have demonstrated improvements in data quality.<sup>20,21</sup> Systems integrating hyperspectral imaging and machine learning have enabled robust iris pigmentation analysis.<sup>7</sup> Studies leveraging convolutional neural networks (CNNs) for gaze tracking and pupil detection have enhanced the accuracy, scalability, and real-time performance of ophthalmic instrumentation.<sup>22,23,24</sup> In our previous study,<sup>4</sup> we compared Expert Systems (ES), Machine Learning (ML), and Deep Learning (DL) algorithms for classifying eye images, with a focus on balancing computational efficiency and classification accuracy to meet the demands of real-time applications. Speed performance proved crucial for modern ophthalmic exams, which require compact, embedded systems capable of real-time operation.<sup>25</sup>

Building on this foundation, we developed *OptoCheck*, a robust solution tailored to overcome key challenges in ophthalmic examinations with enhanced precision and efficiency. Designed for seamless integration, *OptoCheck* is compatible with various ophthalmic devices, including pupillometers, OCT scanners, and corneal topographers,

---

Further author information: (Send correspondence to Giovanni Gibertoni)

E-mail: giovanni.gibertoni@unimore.it

requiring minimal modifications. It achieves precise and high-speed image classification, processing images in just over 1 millisecond on embedded platforms, making it ideal for compact systems and time-sensitive tests. Its cost-effectiveness stems from the use of standard components, including a dichroic mirror, a CMOS camera, and an optical filter, eliminating the reliance on complex algorithms or costly hardware. Beyond its technical simplicity, *OptoCheck* enhances the diagnostic process by providing real-time feedback on eye positioning and patient behavior. This capability enables clinicians to identify uncooperative patients or instances of discomfort during examinations, ensuring accurate and reliable measurements. Ultimately, this innovative approach optimizes ophthalmic test quality, improves clinical workflows, and facilitates faster, more precise diagnoses while maintaining accessibility for widespread adoption.

In the subsequent sections, we detail the design and implementation of *OptoCheck*, followed by experimental validation to demonstrate its effectiveness and applicability in clinical settings.

## 2. MATERIAL AND METHODS

### 2.1 System Design

Figure 1 shows the *OptoCheck* system, comprising three main components: a CMOS camera for imaging, a low-power embedded board for processing, and a Support Vector Machine (SVM) algorithm for real-time classification. These components work together to characterize the *eye state* in real-time by classifying images based on gaze, blink detection, and eye position. The SVM implementation and its detailed performance analysis are extensively described in.<sup>4</sup> The system was integrated into a Maxwellian-View pupillometer,<sup>26,27,28</sup> enabling the accurate acquisition of pupil images through precise alignment and enhanced image processing. The SVM was trained on a publicly available dataset of ocular images (*PopEye*<sup>4</sup>) using features extracted from downsampled  $32 \times 32$  pixel grayscale images, balancing classification accuracy and processing speed for embedded applications on this specific task.

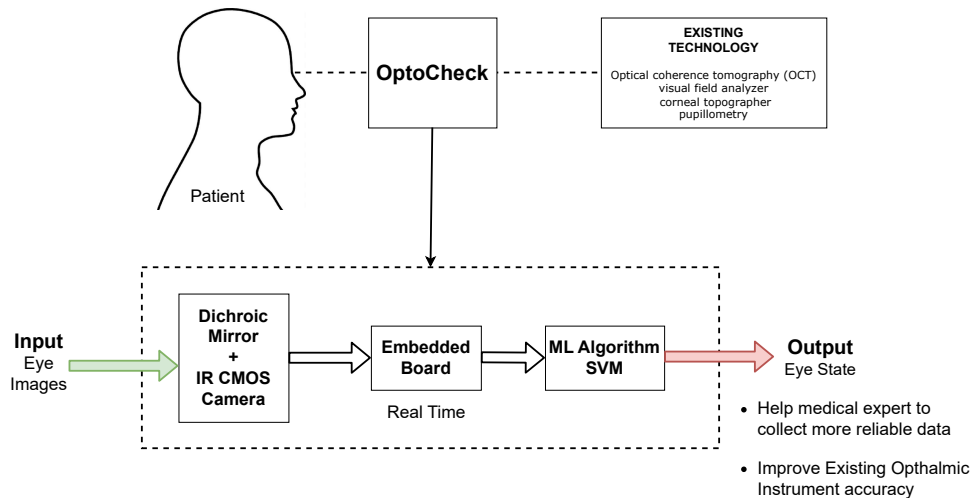


Figure 1: Block diagram of the *OptoCheck* system, highlighting the interaction between the CMOS camera, embedded board, and SVM algorithm. These components work in unison to ensure real-time eye state classification with high efficiency.

The output classification information can be used to trigger visual or auditory alerts when optimal conditions for image acquisition are met, allowing examiners to correct small misalignments or manage non-cooperative patients during examinations promptly.

The optical design illustrated in Figure 2 depicts a modular and compact approach. More specifically, we have used infrared LED light sources (850 nm SFH4250, ams-OSRAM AG, Premstätten, Austria), a 45° dichroic mirror (DMSP750B, Thorlabs, Newton, NJ, USA), and a CMOS camera (BF3-3M-0064ZG-1Y0020

mvBlueFOX3-3M, Matrix Vision GmbH, Germany) mounting a wide angle ( $F = 16\text{mm}$ ) S-Mount lens. A 12 mm high-pass filter ( $\lambda_c = 750\text{nm}$ ) was mounted on the camera to block visible light.

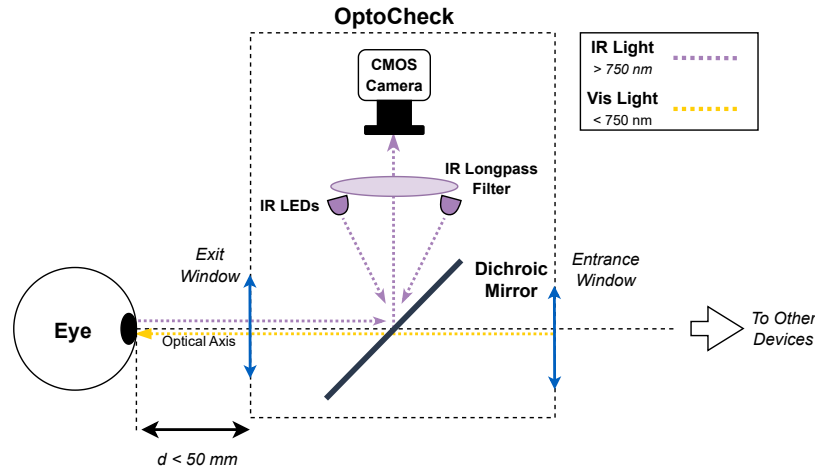


Figure 2: Optical diagram of the *OptoCheck* system. The infrared (IR) light optical path (dashed purple line), using 850 nm SFH4250 LEDs, facilitates eye position monitoring and recording via a CMOS camera (mvBlueFOX3-3M, Matrix Vision GmbH). The visible light optical path (dashed yellow line) is directly transmitted thus allowing eye stimulation. The dichroic mirror (DMSP750B, Thorlabs) separates IR and visible light paths, ensuring compatibility with additional ophthalmic devices.

The use of a dichroic mirror is essential for separating infrared light from visible light, allowing the system to function seamlessly with both new and existing ophthalmic devices without compromising their original functionality. This configuration is highly adaptable; for example, the dichroic mirror can be substituted with one that reflects visible light while transmitting near-infrared (NIR) wavelengths, enabling compatibility with technologies like optical coherence tomography (OCT) scanners that rely on NIR light for precise imaging. The modular and flexible design makes it suitable for a wide range of ophthalmic applications, enhancing both performance and integration potential.

Figure 3 illustrates a 3D design proposal that can be fabricated using any commercially available FDM 3D printer, making it highly customizable for both experimental and professional optical applications. The modular layout has a compact footprint, measuring just 50 mm in the horizontal dimension, and is enclosed within a 50x50x50 mm housing. This design incorporates a dichroic mirror and SMA1 optical windows, featuring standard C-MOUNT internal threading (SM1A10, Thorlabs<sup>©</sup>, Newton, New Jersey, USA).

In most cases, the design can be incorporated into current systems with minimal modifications necessary, whereas in certain situations, it can be seamlessly inserted into the optical path of compatible devices, promoting minimal disruption and facilitating straightforward implementation.

## 2.2 Test Methodology

For preliminary experiments, we have combined the optical design described in the previous Section 2.1 into a Maxwellian-View monocular pupillometer<sup>26,27</sup> integrating a custom four-wavelength LED light source.<sup>28</sup> Preliminary measurements were conducted on eight healthy participants, simulating a typical 2-minute ophthalmic examination involving controlled fixation tasks. During the test, participants were instructed to fixate on a circular red target while seated comfortably on a clinical chin rest. Moreover, the red light stimulation was configured to have a  $20.5^\circ$  FOV and  $120\text{ cd/m}^2$  with peak wavelength at 630 nm and 14 nm FWHM. The camera was configured to acquire images with fixed frame rate equal to 50 Hz. The eye sample images, illustrated in Figure 4, were pre-processed and categorized into one of six classes: ‘correct’, ‘closed’, ‘right’, ‘down’, ‘left’, and

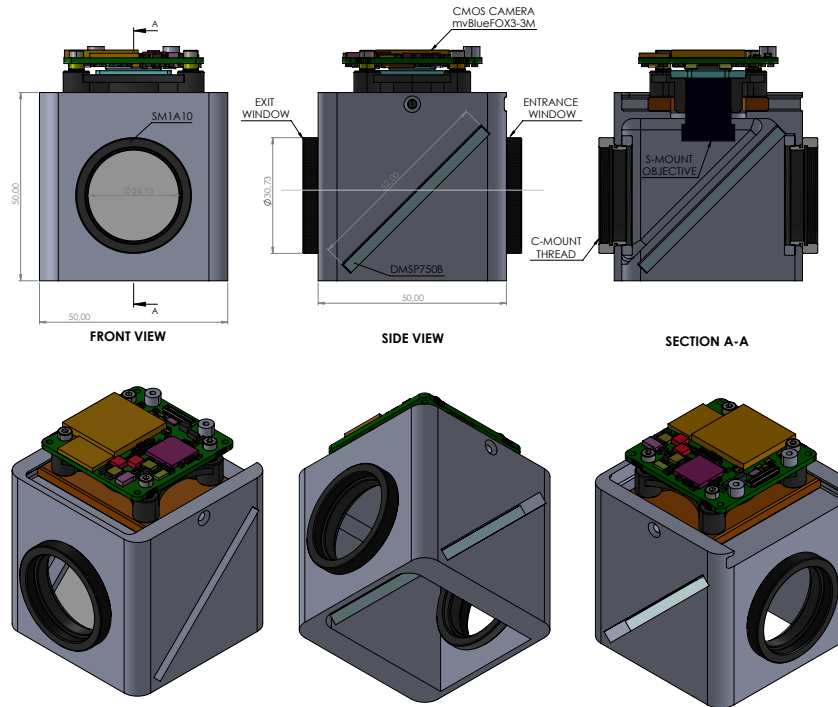


Figure 3: Illustration of the modular integration design for the mvBlueFOX3-3M CMOS camera. The system features C-mount threads for easy attachment to optical instruments, an entrance and exit window for optical paths, and compatibility with the SM1A10 adapter for enhanced modularity. The side view, front view, and cross-sectional view (A-A) highlight the dimensions and internal configuration, including the integration of the DMS P750B (Thorlabs © Newton, New Jersey, U.S.) dichroic mirror optics and S-mount objective.

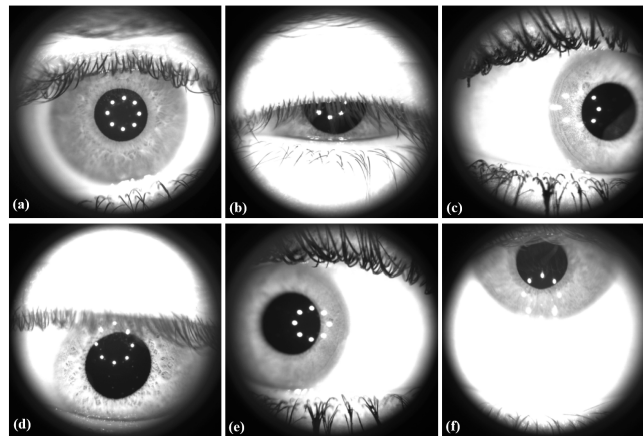


Figure 4: Example images classified into six categories: a) correct b) closed c) right d) down e) left f) up.

‘up’. These categories were selected to address typical challenges in pupillometry, including off-axis gaze and partial eyelid closure.

These classes have been purposefully chosen for pupillometry assessments, in which the measurement of pupil size conducted by conventional image processing techniques may be affected by an off-axis gaze or a partly closed eyelid. It is significant to note that this approach can be used for different kinds and amounts of categories, including blurred or sharp images, partial or complete blinks, or inadequate image exposure, tailored to the specific application task. As we have described in our previous work<sup>4</sup> the Support Vector Machine (SVM) algorithm with  $32 \times 32$  pixel normalized and unrolled input size images demonstrated the best balance of accuracy and speed as it achieved 96.2% prediction accuracy with an average 1.7 ms Single Frame Prediction Time (SFPT)

on a 10 Watt Cortex A53 CPU.

In this particular research, a Python-driven image processing technique<sup>27,29</sup> was employed to determine the pupil’s position and size, while the SVM algorithm was utilized for detecting partial blinks throughout the experiment. In the results section, we were interested in identifying both complete blinks—when the eyelid is fully closed and the pupil becomes undetectable—and partial blinks, where the eyelid is partially closed, potentially obscuring the pupil and compromising the accuracy of pupil size measurements<sup>30</sup> (Figure 5).

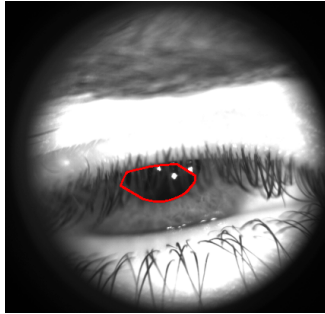


Figure 5: Figure illustrates pupil detection using an image processing algorithm designed to estimate pupil size even with a partially closed eyelid. The red perimeter highlights the detected pupil region. Standard methods such as ellipse fitting and minimum enclosing circle fail to provide an accurate measurement of pupil size due to partial occlusion by the eyelid.

Blink frequency and duration are critical indicators of patient discomfort or fatigue, which can affect measurement reliability and compromise the pupillary response.<sup>31</sup> This dual focus on both the detection of partial and complete blinks and the analysis of blinking behavior adds an additional layer of diagnostic insight, aiding in the evaluation of the patient’s physiological and psychological state during the examination.

## RESULTS AND DISCUSSION

Our analysis of blinking behavior revealed key patterns of variability and their potential impact on ophthalmic imaging reliability. The average blink duration observed among the eight participants was 190 milliseconds, with an average blink rate of 13 blinks per session. These findings are summarized in Table 1, which provides detailed participant-specific data. While the average measured blink rate is significantly lower than reported values of 14 to 17 blinks per minute under normal conditions,<sup>32,33</sup> variability between participants reflects individual factors such as discomfort, dryness, or task-induced stress. Notably, other studies, such as,<sup>34</sup> have shown that blink rates are strongly influenced by the nature of the task, with cognitively demanding or visually intensive tasks often associated with reduced blink frequencies.

Table 1: Summary of blink behavior across participants. The table highlights variability in blink frequency and duration, which may reflect individual differences in comfort and task engagement.

Patient	Number of Blinks	Average Blink Duration (s)
0	17	0.10
1	10	0.20
2	26	0.40
3	24	0.12
4	8	0.12
5	7	0.12
6	8	0.32
7	5	0.22

Figure 6 shows the distribution of blink durations. Most blinks fell within the range of 0.10 to 0.15 seconds, consistent with prior studies on spontaneous blinking behavior.<sup>32,33</sup>

These results demonstrate the effectiveness of the *OptoCheck* system in accurately detecting and classifying blinks in real-time. By excluding frames affected by excessive blinking or partial occlusions, the system ensures reliable data acquisition. This aligns with previous research highlighting the importance of robust methodologies

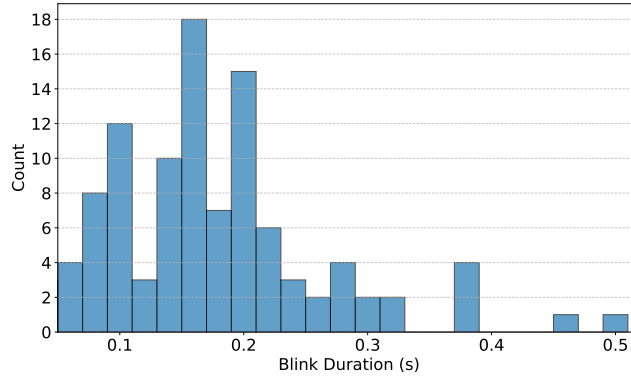


Figure 6: Histogram showing the distribution of blink durations. The x-axis represents the blink duration in seconds, grouped into intervals of 20 ms, while the y-axis indicates the count of occurrences for each interval.

in ophthalmic imaging. Notably, the data also highlight that some patients exhibited significantly more frequent blinking compared to others, potentially indicating greater difficulty in completing the task. This variability could be explained by factors such as dryness, light sensitivity, stress, discomfort, or lack of familiarity with the test. These conditions may lead to increased blinking and present additional challenges in maintaining stable measurements, further underlining the utility of *OptoCheck* in such scenarios.

Monitoring the pupil’s position during the test can be particularly valuable for evaluating patient compliance and focus. Observing deviations from the central area within the framed region can help identify whether the patient is distracted, struggling to maintain fixation on the target, or experiencing discomfort. Such insights are critical for ensuring the reliability of the measurements, as they allow for the detection of non-compliance or shifts in attention. By addressing these deviations, clinicians can make necessary adjustments to improve test conditions, ultimately enhancing data quality and patient experience. In our test case, the analysis of pupil positions, shown in Fig. 7, highlights the distribution of normalized X and Y coordinates during the experiment. A total of 42,701 data points containing pupil position were collected during the experiments. The majority of the data points are concentrated around the center of the image, indicating that the eye remained predominantly central during the experiment. Ellipses representing 68%, 95%, and 99.7% confidence levels were overlaid to further emphasize the distribution of the data. The equivalent diameters of these ellipses were calculated as 1.73 mm, 2.80 mm, and 3.90 mm, respectively. These results likely reflect that the test, involving fixation on a single spot of uniform red light, was relatively simple for most participants, resulting in a stable, central position of the detected pupil.

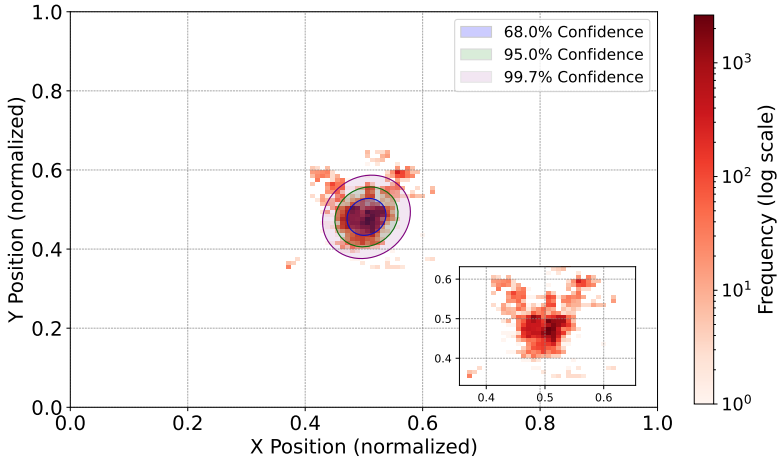


Figure 7: Distribution of pupil positions during the experiment. The plot shows the normalized X and Y positions of the pupil inside the Field of View of the camera. Most data points are concentrated at the center, reflecting stable fixation.

Notably, in this specific test, participants were instructed to look at the red fixation area. As a result, no frames where the pupil moved significantly up, down, left, or right were detected by the SVM algorithm. However, in other types of tests where a fixation target is absent, or in conditions such as darkness where the pupil might move more erratically, the patient’s eye could exhibit significantly greater deviations. In such scenarios, the classification algorithm would be particularly useful for identifying images where the eye is substantially misaligned with the optical axis or where the gaze is incorrect. Looking at Figure 7, the presence of a few distant outliers highlights the potential challenges in maintaining reliable measurements for patients with unstable fixation. The robust classification algorithm of *OptoCheck* helps identify and exclude these frames, ensuring data integrity. This further underscores the importance of robust classification to ensure accurate identification and exclusion of frames where the pupil’s position or gaze deviates excessively.

Incorporating these capabilities into routine ophthalmic examinations, particularly for non-cooperative patients, enhances data quality and reduces diagnostic errors. Future work will aim to expand testing to diverse populations and explore integration with other ophthalmic devices, further advancing the reliability and efficiency of diagnostic imaging.

## CONCLUSIONS

Integrating *OptoCheck* into ophthalmic devices can enhance diagnostic accuracy and improve patient outcomes. By addressing key challenges, such as non-cooperative patients and involuntary eye movements, this technology marks a significant step forward in ophthalmic instrumentation. The system enables more precise and efficient examinations by providing real-time feedback on eye positioning and patient behavior, reducing measurement errors and minimizing examination times. These capabilities not only streamline clinical workflows but also ensure more reliable diagnoses and tailored patient care.

The results of our study demonstrate the system’s ability to accurately detect and classify blink behaviors and pupil positions, even under challenging conditions. This highlights its applicability in diverse clinical scenarios, from routine examinations to research settings.

Future developments will aim to integrate the system with additional ophthalmic devices while expanding its applications to include blur detection, optimizing image exposure, and assessing stress or fatigue. Furthermore, validating the system’s performance on larger and more diverse populations will enhance its reliability and applicability. With these advancements, *OptoCheck* has the potential to establish new benchmarks for precision, efficiency, and accessibility in the diagnosis and management of eye diseases.

## ACKNOWLEDGMENTS

The authors would like to thank Guido Borghi from the University of Modena and Reggio Emilia for his invaluable assistance with algorithm selection, including the implementation of the Support Vector Machine (SVM), testing alternative classification algorithms, and optimizing processing speed for embedded systems. We also extend our gratitude to Behrad Garmsiri from the State University of New York (SUNY) College of Optometry in New York City for his insightful discussions and suggestions, which significantly inspired this work.

## REFERENCES

- [1] dos Santos, E. S., Xavier, W. B., Rodrigues, R. N., da C. Botelho, S. S., and Werhli, A. V., “Vision based measurement applied to industrial instrumentation,” *IFAC-PapersOnLine* **50**(1), 788–793 (2017). 20th IFAC World Congress.
- [2] Fedullo, T., Cassanelli, D., Gibertoni, G., Tamarin, F., Quaranta, L., Riva, I., Tanga, L., Oddone, F., and Rovati, L., “Assessment of a Vision-Based Technique for an Automatic Van Herick Measurement System,” *IEEE Transactions on Instrumentation and Measurement* **71**, 1–11 (2022). Conference Name: IEEE Transactions on Instrumentation and Measurement.
- [3] Gallagher, C. V., Bruton, K., Leahy, K., and O’Sullivan, D. T., “The suitability of machine learning to minimise uncertainty in the measurement and verification of energy savings,” *Energy and Buildings* **158**, 647–655 (2018).
- [4] Gibertoni, G., Borghi, G., and Rovati, L., “Vision-Based Eye Image Classification for Ophthalmic Measurement Systems,” *Sensors* **23**, 386 (Jan. 2023).

- [5] Yao, T., Qu, C., Liu, Q., Deng, R., Tian, Y., Xu, J., Jha, A., Bao, S., Zhao, M., Fogo, A. B., Landman, B. A., Chang, C., Yang, H., and Huo, Y., “Compound Figure Separation of Biomedical Images with Side Loss,” in [*Deep Generative Models, and Data Augmentation, Labelling, and Imperfections*], Engelhardt, S., Oksuz, I., Zhu, D., Yuan, Y., Mukhopadhyay, A., Heller, N., Huang, S. X., Nguyen, H., Sznitman, R., and Xue, Y., eds., *Lecture Notes in Computer Science*, 173–183, Springer International Publishing, Cham (2021).
- [6] Kim, S. J., Cho, K. J., and Oh, S., “Development of machine learning models for diagnosis of glaucoma,” *PLOS ONE* **12**, e0177726 (may 2017).
- [7] Fedullo, T., Masetti, E., Gibertoni, G., Tramarin, F., and Rovati, L., “On the Use of an Hyperspectral Imaging Vision Based Measurement System and Machine Learning for Iris Pigmentation Grading,” in [*2022 IEEE International Instrumentation and Measurement Technology Conference (I2MTC)*], 1–6 (may 2022). ISSN: 2642-2077.
- [8] Daniel Shu Wei Ting, M., “Development and Validation of a Deep Learning System for Diabetic Retinopathy and Related Eye Diseases Using,” *JAMA* **318**, 2211–2223 (Dec 2017).
- [9] Balyen, L. and Peto, T., “Promising Artificial Intelligence-Machine Learning-Deep Learning Algorithms in Ophthalmology,” *The Asia-Pacific Journal of Ophthalmology* **8**, 264–272 (Jun 2019).
- [10] Shimizu, E., Yazu, H., Aketa, N., Yokoiwa, R., Sato, S., Yajima, J., Katayama, T., Sato, R., Tanji, M., Sato, Y., Ogawa, Y., and Tsubota, K., “A Study Validating the Estimation of Anterior Chamber Depth and Iridocorneal Angle with Portable and Non-Portable Slit-Lamp Microscopy,” *Sensors* **21**(4), 1436 (2021).
- [11] Cassanelli, D., Fedullo, T., Gibertoni, G., Saporito, G., Ferrazza, M., Oddone, F., Riva, I., Quaranta, L., Tramarin, F., and Rovati, L., “Training of an artificial intelligence algorithm for automatic detection of the Van Herick grade,” in [*Ophthalmic Technologies XXXII*], **11941**, 35–41, SPIE (Mar. 2022).
- [12] Cassanelli, D., Gibertoni, G., Cattini, S., Quaranta, L., Riva, I., Bruttini, C., De Angelis, G., and Rovati, L., “A new screening system for the estimation of ocular anterior chamber angle width,” in [*Ophthalmic Technologies XXXI*], **11623**, 101–105, SPIE (2021).
- [13] Rong, Y., Xiang, D., Zhu, W., Yu, K., Shi, F., and Fan, Z., “Surrogate-Assisted Retinal OCT Image Classification Based on Convolutional Neural Networks,” *IEEE J. Biomed. Health Inf.* **23**, 253–263 (Feb. 2018).
- [14] Saleh, G. A., Batouty, N. M., Haggag, S., Elnakib, A., Khalifa, F., Taher, F., Mohamed, M. A., Farag, R., Sandhu, H., Sewelam, A., and El-Baz, A., “The Role of Medical Image Modalities and AI in the Early Detection, Diagnosis and Grading of Retinal Diseases: A Survey,” *Bioengineering* **9**, 366 (Aug. 2022).
- [15] Gibertoni, G., Hromov, A., Piffaretti, F., and Geiser, M. H., “Development of an Innovative Pupillometer Able to Selectively Stimulate the Eye’s Fundus Photoreceptor Cells,” *Diagnostics* **14**, 1940 (Jan. 2024).
- [16] Sawada, A., Yamada, H., Yamamoto, Y., and Yamamoto, T., “Intraocular pressure alterations after visual field testing,” *Jpn. J. Ophthalmol.* **58**, 429–434 (Sept. 2014).
- [17] Bertaud, S., Skarbek Borowski, E., Abbas, R., Baudouin, C., and Labbé, A., “Influence of automated visual field testing on intraocular pressure,” *BMC Ophthalmol.* **20**, 1–6 (Dec. 2020).
- [18] Fedullo, T., Cassanelli, D., Gibertoni, G., Tramarin, F., Quaranta, L., de Angelis, G., and Rovati, L., “A Machine Learning Approach for a Vision-Based Van-Herick Measurement System,” in [*2021 IEEE International Instrumentation and Measurement Technology Conference (I2MTC)*], 1–6 (May 2021).
- [19] Cao, X., “Eye Tracking in Human-computer Interaction Recognition,” in [*2023 IEEE International Conference on Sensors, Electronics and Computer Engineering (ICSECE)*], 1–5 (2023).
- [20] Cech, J. and Soukupova, T., “Real-time eye blink detection using facial landmarks,” tech. rep., Center for Machine Perception, Department of Cybernetics, Faculty of Electrical Engineering, Czech Technical University, Prague (2016).
- [21] Agarwal, M. and Sivakumar, R., “Blink: A Fully Automated Unsupervised Algorithm for Eye-Blink Detection in EEG Signals,” in [*2019 57th Annual Allerton Conference on Communication, Control, and Computing (Allerton)*], 1113–1121 (sep 2019).
- [22] Krafska, K., Khosla, A., Kellnhofer, P., Kannan, H., Bhandarkar, S., Matusik, W., and Torralba, A., “Eye tracking for everyone,” in [*Proceedings of the IEEE conference on computer vision and pattern recognition*], 2176–2184 (2016).
- [23] Vera-Olmos, F. J., Pardo, E., Melero, H., and Malpica, N., “DeepEye: Deep convolutional network for pupil detection in real environments,” *Integrated Computer-Aided Engineering* **26**, 85–95 (jan 2019).
- [24] Khan, W., Hussain, A., Kuru, K., and Al-askar, H., “Pupil Localisation and Eye Centre Estimation Using Machine Learning and Computer Vision,” *Sensors* **20**, 3785 (Jan 2020). Number: 13 Publisher: Multidisciplinary Digital Publishing Institute.
- [25] Lee, J., Stanley, M., Spanias, A., and Tepedelenioglu, C., “Integrating machine learning in embedded sensor systems for internet-of-things applications,” in [*2016 IEEE international symposium on signal processing and information technology (ISSPIT)*], 290–294, IEEE (2016).
- [26] Gibertoni, G., Pinto, V. D., Cattini, S., Tramarin, F., Geiser, M., and Rovati, L., “A simple Maxwellian optical system to investigate the photoreceptors contribution to pupillary light reflex,” in [*Ophthalmic Technologies XXXII*], **11941**, 52–60, SPIE (mar 2022).
- [27] Gibertoni, G., Irungovel, A. B. P., Viswanathan, S., and Rovati, L., “Silent stimulation of cones: A comparison between the ERG and PLR responses,” in [*Ophthalmic Technologies XXXIII*], **12360**, 156–166, SPIE (Mar. 2023).

- [28] Gibertoni, G., Borghi, G., and Rovati, L., “Compact High-Resolution Multi-Wavelength LED Light Source for Eye Stimulation,” *Electronics* **13**, 1127 (Jan. 2024).
- [29] Gibertoni, G., Cattini, S., and Rovati, L., “Towards the development of a new model for the oculomotor system,” in [*Ophthalmic Technologies XXXI*], **11623**, 93–100, SPIE (Mar. 2021).
- [30] Grootjen, J. W., Weingärtner, H., and Mayer, S., “Highlighting the challenges of blinks in eye tracking for interactive systems,” in [*Proceedings of the 2023 Symposium on Eye Tracking Research and Applications*], Article 63, 7 pages (2023).
- [31] Yang, B., Intoy, J., and Rucci, M., “Eye blinks as a visual processing stage,” *Proceedings of the National Academy of Sciences* **121**(15), e2310291121 (2024).
- [32] Blount, W., “Studies of the movements of the eyelids of animals: blinking,” *Quarterly Journal of Experimental Physiology* **18**(2), 111–125 (1927).
- [33] Bentivoglio, A. R., Bressman, S. B., Cassetta, E., Carretta, D., Tonali, P., and Albanese, A., “Analysis of blink rate patterns in normal subjects,” *Mov. Disord.* **12**, 1028–1034 (Nov. 1997).
- [34] Doughty, M. J., “Consideration of Three Types of Spontaneous Eyeblink Activity in Normal Humans: during Reading and Video Display Terminal Use, in Primary Gaze, and while in Conversation,” *Optom. Vis. Sci.* **78**, 712 (Oct. 2001).